J Shoulder Elbow Surg (2019) 28, 1316–1325

ELSEVIER

Journal of Shoulder and Elbow Surgery

www.elsevier.com/locate/ymse

Coracoacromial morphology: a contributor to recurrent traumatic anterior glenohumeral instability?

Matthijs Jacxsens, MD[a,b], Shireen Y. Elhabian, PhD[c], Sarah E. Brady, BS[d], Peter N. Chalmers, MD[a], Robert Z. Tashjian, MD[a], Heath B. Henninger, PhD[a,c,d,*]

[a]*Department of Orthopaedics, University of Utah, Salt Lake City, UT, USA*
[b]*Department of Orthopaedics and Traumatology, Kantonsspital St. Gallen, St. Gallen, Switzerland*
[c]*Scientific Computing and Imaging Institute, School of Computing, University of Utah, Salt Lake City, UT, USA*
[d]*Department of Bioengineering, University of Utah, Salt Lake City, UT, USA*

Background: Although scapular morphology contributes to glenohumeral osteoarthritis and rotator cuff disease, its role in traumatic glenohumeral instability remains unknown. We hypothesized that coracoacromial and glenoid morphology would differ between healthy subjects and patients with recurrent traumatic anterior shoulder instability.

Methods: Computed tomography scans of 31 cadaveric control scapulae and 54 scapulae of patients with recurrent traumatic anterior shoulder instability and Hill-Sachs lesions were 3-dimensionally reconstructed. Statistical shape modeling identified the modes of variation between the scapulae of both groups. Corresponding measurements quantified these modes in relation to the glenoid center (linear offset measures), defined by the best-fit circle of the inferior glenoid, or the glenoid center plane (angles), which bisects the glenoid longitudinally. Distances were normalized for glenoid size.

Results: Compared with controls, the unstable coracoids were shorter ($P = .004$), with a more superior and medial offset of the tip (mean difference [MD], 7 and 3 mm, respectively; $P < .001$) and an origin closer to the 12-o'clock position (MD, 6°; $P < .001$). The unstable scapular spines originated closer to the 9-o'clock position (MD, 4°; $P = .012$), and the unstable acromions were more vertically oriented (MD, 6°; $P < .001$). The unstable glenoids had an increased height-width index (MD, 0.04; $P = .021$), had a flatter anterior-posterior radius of curvature (MD, 77 mm; $P < .001$), and were more anteriorly tilted (MD, 5°; $P = .005$).

Conclusions: Coracoacromial and glenoid anatomy differs between individuals with and without recurrent traumatic anterior shoulder instability. This pathologic anatomy is not addressed by current soft-tissue stabilization procedures and may contribute to instability recurrence.

Ethical approval for this study was obtained from the University of Utah Institutional Review Board (Nos. 17182 and 92668).

*Reprint requests: Heath B. Henninger, PhD, Department of Orthopaedics, Orthopaedic Research Laboratory, University of Utah, 590 Wakara Way, Room A0100, Salt Lake City, UT 84108, USA.
E-mail address: heath.henninger@utah.edu (H.B. Henninger).

1058-2746/$ - see front matter
https://doi.org/10.1016/j.jse.2019.01.009

Level of evidence: Level III; Case-Control Design; Prognosis Study

Keywords: Shoulder instability; Hill-Sachs; scapular morphology; acromion morphology; coracoid morphology; glenoid morphology; shape modeling; 3D reconstruction

The glenohumeral joint (GHJ) is the most frequently dislocated joint in the body.[24] The majority of GHJ dislocations are traumatic anterior dislocations.[32] Glenohumeral instability is frequently recurrent (up to 85% within 5 years in young male patients), leads to functional impairment, and can cause degenerative changes.[8,35] Traumatic anterior shoulder dislocations are associated with capsulolabral-ligamentous tears, glenoid rim fractures, and posterosuperior humeral head compression fractures.[32] The risk factors for recurrence with operative and nonoperative treatment have been well described and include defects of the anterior glenoid rim,[6,28,30,37] and large humeral-sided bony lesions called Hill-Sachs lesions,[18] as well as combinations thereof.[34,36]

However, few studies have addressed osseous morphologic factors that may contribute to recurrent traumatic anterior shoulder instability beyond anteroinferior glenoid rim lesions and posterosuperior humeral head lesions. For instance, a taller, narrower, and flatter glenoids may be associated with recurrence.[29,31,33] Glenoid version has been debated: Hohmann and Tetsworth[17] and Aygün et al[3] found increased anteversion whereas Moroder et al[29] and Peltz et al[33] found no difference in glenoid version when comparing patients with recurrent traumatic instability and healthy subjects.

The anatomy of the coracoacromial (CA) arch may also contribute to the etiology of recurrent traumatic anterior glenohumeral instability. Owens et al[31] identified the coracohumeral distance as an independent risk factor for traumatic anterior instability, with a 20% increased risk of instability for every 1-mm increase in coracohumeral distance. Anatomic differences between individuals with and without recurrent traumatic anterior glenohumeral instability have implications for understanding the etiology of, risk factors for, possible preventions for, and mechanisms for treatment of recurrent traumatic anterior glenohumeral instability.

The aim of this study was to quantify and compare glenoid and periarticular scapular morphology between healthy shoulders and those with recurrent traumatic anterior shoulder instability. It was hypothesized that both glenoid morphology and periarticular scapular anatomy would be different between healthy subjects and patients with recurrent anterior shoulder instability.

Methods

Study population

In this anatomic case-control study, a retrospective review of patients who underwent procedures for anterior shoulder instability between 2008 and 2016 was performed. Skeletally mature patients with recurrent traumatic anterior shoulder instability (≥2 dislocation events) and an osseous Hill-Sachs lesion visible on computed tomography (CT) scans without contrast were included. The presence of an osseous Hill-Sachs lesion provided proof of a definite anterior shoulder dislocation. The exclusion criteria were the presence of concomitant lesions, instability secondary to seizures or hyperlaxity, degenerative changes of the GHJ, and poor-quality CT scans. A retrospective review of electronic medical records and surgery reports identified the preoperative baseline demographic characteristics of the subjects, mechanism of the first dislocation (traumatic vs. atraumatic), number of dislocations, preoperative clinical and radiographic findings, intraoperative findings, and procedures performed. This study group was labeled the "unstable group." The control group included cadaveric scapulae from an existing database, verified to be free of any shoulder pathology as seen by an orthopedic surgeon during dissection and on CT scans.

Imaging protocol

The instability patients and cadaveric controls underwent CT scans acquired using a Siemens Somatom CT scanner (Siemens Medical, Malvern, PA, USA) (130 kV, 512 × 512 matrix, 2.0-mm [unstable group] or 1.0-mm [control group] slice thickness, 0.75 pitch, and current of 170 milliampere-seconds). Clinical CT data sets were upsampled to axial slice thicknesses of 1.0 mm to improve resolution. All images were exported into DICOM (Digital Imaging and Communications in Medicine) format and reconstructed into 3-dimensional (3D) surfaces using semiautomatic segmentation techniques (Mimics; Materialise, Leuven, Belgium).

Statistical shape modeling

Computationally derived statistical shape modeling (SSM) approaches are useful to objectively quantify population-level shape variation and anatomic differences, independent of size differences between subjects.[2,16] In particular, point-based correspondence models are the computational extension of manual landmark application that enable the automatic dense placement of homologous landmarks on 3D models of anatomy, offering more detailed anatomic geometric representations and capturing more subtle shape variations than traditional landmark-based approaches. In this regard, the validated SSM software ShapeWorks[9] was used to identify the modes of variation and to detect differences between the mean shape of the control and pathologic scapulae, without idealizing underlying geometry. Without relying on any surface parameterization, ShapeWorks computes a statistically optimal representation of the population variability by choosing landmark

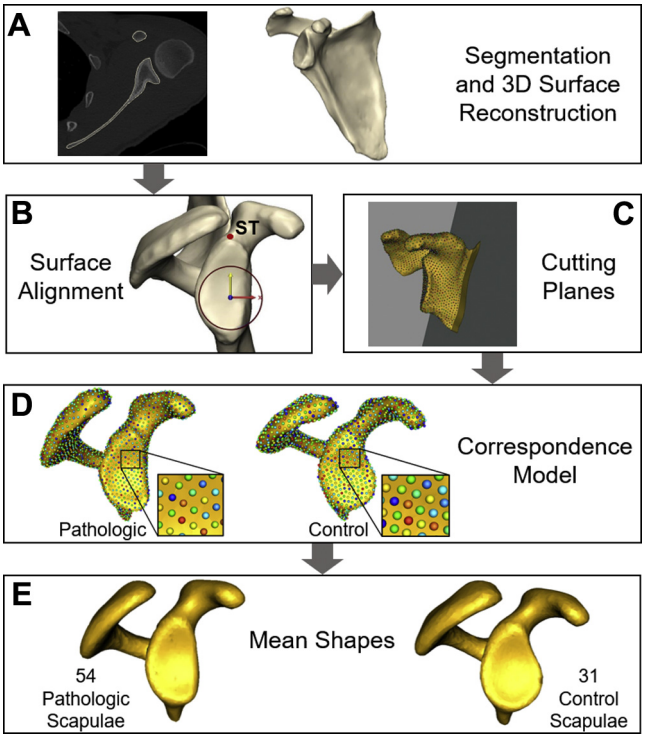

Figure 1 Computational flowchart to generate mean shapes in control and unstable groups to evaluate for shape differences. **(A)** Computed tomography scans were semiautomatically segmented and 3-dimensionally reconstructed. All left scapulae were mirrored to a right scapula. **(B)** Three-dimensional (*3D*) surfaces were aligned to a glenoid-based coordinate system with the center of the best-fit circle to the inferior glenoid as the origin, the glenoid circle defining the X-Y plane, and the Y-Z plane (glenoid center plane) defined as the plane perpendicular to the glenoid circle, containing the center of the glenoid circle and the supraglenoid tubercle (*ST*). **(C)** To focus the analysis on the periarticular anatomy, a cutting plane was created through the scapular notch, parallel to the glenoid circle. **(D)** A total of 2048 correspondence points were hierarchically placed on the region of interest. **(E)** Statistical shape modeling created the mean shapes in both groups.

positions (ie, correspondence points) that minimize the overall information content of the model while maintaining a good sampling of surface geometry.

During preprocessing, left scapulae were mirrored to a right scapula and all 3D surfaces were aligned to a glenoid-based coordinate system (3-matic; Materialise) (Fig. 1).[20] To focus the analysis on the periarticular anatomy of the scapula and concentrate placement of correspondence points on the region of interest, a cutting plane was defined through the scapular notch parallel to the best-fit circle of the inferior glenoid. A total of 2048 correspondence points were hierarchically placed on the region of interest and used to generate the mean shape of both groups. The difference between mean shapes provided a mode-based and visual assessment that guided the selection of morphometric measurements for analysis (Fig. 2, Video S1).

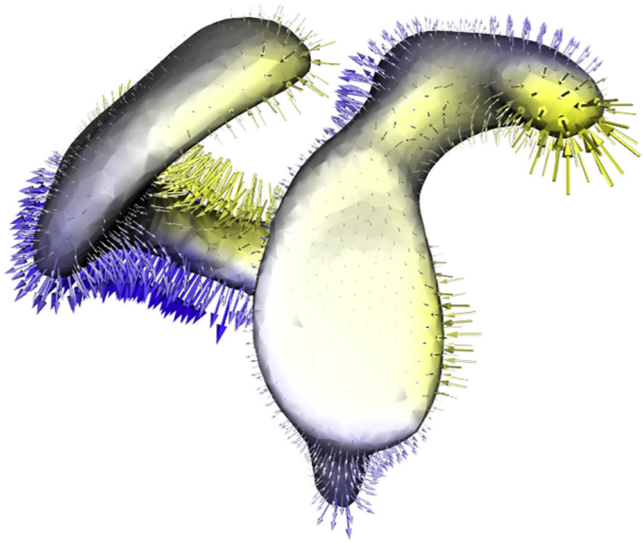

Figure 2 Statistical shape modeling determined the group differences between the mean control and mean pathologic unstable scapulae. The *blue arrows* indicate an increase and the *yellow arrows* denote a decrease in the morphologic difference between the illustrated mean control shape and the mean unstable shape, with the size of the arrow indicative of the magnitude of the difference. Compared with the mean control shape, the mean pathologic shape demonstrated a posteriorly tilted coracoid pillar and scapular spine, an anterosuperiorly oriented and shorter coracoid with a more vertical orientation of the acromion, and a more posteriorly rotated coracoacromial arch and coracoacromial base. Additional shape variation was seen at the inferior and anterior glenoid rim. This analysis guided morphometric measurements.

Morphometrics

To quantify the morphologic differences between groups, each scapula was imported into 3-matic, and measurements focused on the regions highlighted by the modes of variation (Fig. 3). The center of the best-fit circle of the inferior glenoid and the glenoid center plane were used as references for offset and angle measurements, respectively. Angles were measured in the plane of the glenoid unless noted otherwise. Absolute distances between landmarks were assessed and also normalized to the radius of the glenoid circle to compensate for differences in absolute size between scapulae.

Periarticular measures included the anterior, superior, and lateral offset of the apex and base of the coracoid process as defined by Chahla et al.[10] The apex and base of the coracoid determined the coracoid length and coracoid deviation angle, measured in the transverse plane. The coracoid pillar angle was acquired using the best-fit plane through the middle of the pillar. Similarly, the best-fit plane through the middle of the base of the acromion determined the scapular spine angle. The orientation of the best-fit plane of the acromion undersurface defined acromial tilting. The CA relationship was acquired by assessing the distance between the coracoid apex and the anterolateral corner of the acromion (CA arch length), as well as the posterolateral corner

of the acromion (CA base length). These 2 line segments further defined the CA arch angle and CA base angle.

Glenoid measures involved the anterior-posterior (AP) radius of curvature (ROC) of the posterior segment of the articular surface, the superior-inferior ROC of the articular surface, the height-width (H-W) index of the glenoid face, and the calculation of glenoid bone loss as described by Bhatia et al.[5] The defect chord in relation to the glenoid center plane determined glenoid defect orientation.

The scapular axis, defined by the point where the scapular spine intersects the medial border of the scapula at the trigonum scapulae and the center of the glenoid circle, and the scapular plane, defined by the scapular axis and the most inferior point of the inferior angle of the scapula, were used to determine the glenoid relationship to the scapula. Glenoid version was defined as 90° minus the angle between the scapular plane and the glenoid circle, with a negative value representing retroversion. The angle between the scapular plane and the glenoid center plane defined glenoid anterior tilting. The angle between the scapular axis and the line connecting the most lateral point of the superior and inferior glenoid pole in the coronal plane provided glenoid inclination.

Statistical analysis

Data normality was verified by the Shapiro-Wilk test. A 2-tailed Student *t* test and Mann-Whitney *U* test were used for comparison, as appropriate. To determine the reliability of the measurements, 2 investigators (M.J. and S.E.B.) assessed each measurement independently on 15 control and 15 pathologic scapulae. One investigator (M.J.) repeated all measurements after a minimum time interval of 2 weeks. Reliability was quantified using the intraclass correlation coefficient and typical error of measurement. The interpretation of intraclass correlation coefficients was as follows: 0.40 or less, poor; 0.401 to 0.600, fair; 0.601 to 0.750, good; and 0.751 to 1.000, excellent.[12] Statistical tests were conducted at a significance level of $P \leq .05$. Analyses were performed with SPSS Statistics software (version 24.0; IBM, Armonk, NY, USA).

Results

Between 2008 and 2016, 307 patients underwent procedures for anterior shoulder instability at our institution. A total of 74 patients met the inclusion criteria. We excluded 10 patients because of instability secondary to seizures, 4 who had a CT scan with poor quality, 2 who had degenerative changes, 1 who had laxity, and 3 who had a concomitant lesion. This left a final study population in the unstable group of 54 shoulders (19 right and 35 left) in 54 patients (46 men and 8 women) with an average age of 28 years (range, 18-50 years). Anterior capsulolabral repair was performed in 26, of whom 3 underwent an additional remplissage procedure. The Latarjet procedure was performed in 28 subjects. The control group consisted of 31 shoulders (16 right and 15 left) in 31 cadavers (16 male and 15 female cadavers) with an average age of 60 years (range, 40-78 years).

When morphology differences between mean shapes were compared, qualitative observation demonstrated a large shape variation around the periarticular anatomy and the anterior-inferior glenoid (Fig. 2, Video). With qualitative observation, the orientation of the scapular spine and acromion differed the most with a more posteriorly rotated scapular spine, approximating the 9-o'clock position, and a more vertical acromion in the unstable group. The mean shape of the coracoid process in the unstable group was more medially and superiorly oriented with a posteriorly rotated coracoid pillar closer to the 12-o'clock position than the 3-o'clock position. The glenoid in the unstable group was larger at the inferior pole with a shape variation at the anterior glenoid rim corresponding with the glenoid defect.

The quantitative morphometric analysis revealed that the unstable group had a larger superior and medial offset of the apex of the coracoid process (mean difference, 7 and 3 mm, respectively; $P < .001$) (Table I, Fig. 4). The base of the coracoid was more medially and posteriorly oriented in the unstable group (mean difference, 3 mm for both measures; $P < .001$). Although the absolute measure did not differ ($P = .857$), the normalized measurement revealed a more inferior orientation of the coracoid base in the pathologic group ($P = .029$). This led to a larger coracoid deviation angle (mean difference, 3°; $P = .013$) (Table II) and a shorter normalized coracoid length in patients with anterior instability ($P = .004$). Compared with controls, the unstable group had a more posteriorly rotated coracoid pillar, more posteriorly rotated scapular spine, and more vertical acromial tilt (mean difference, 6°, 4°, and 6°, respectively; $P < .001$, $P = .012$, and $P < .001$, respectively). These differences around the coracoid and acromion led to a more horizontal orientation of the CA arch and more vertical orientation of the CA base (mean difference, 9°; $P < .001$). The larger absolute CA arch and base length of the pathologic group did not correspond to a difference in normalized length ($P = .036$ vs. $P = .945$ and $P < .001$ vs. $P = .543$, respectively).

Compared with the control subjects, the glenoids in the pathologic group had an increased estimated H-W index (1.40 vs. 1.44, $P = .021$) and were flatter in the AP direction (AP ROC, 58 mm vs. 135 mm; $P < .001$) (Table III). No differences in the superior-inferior ROC (35 mm vs. 37 mm, $P = .069$), glenoid version (1° vs. 2°, $P = .114$), and inclination (84° vs. 86°, $P = .155$) were found. The glenoid was more anteriorly tilted in the pathologic group (mean difference, 5°; $P = .005$). Mean glenoid bone loss was 14% ± 7% with a mean defect orientation of 1° ± 8°. The reliability of the measurements for both inter-rater and intrarater observations was good to excellent (Table S1).

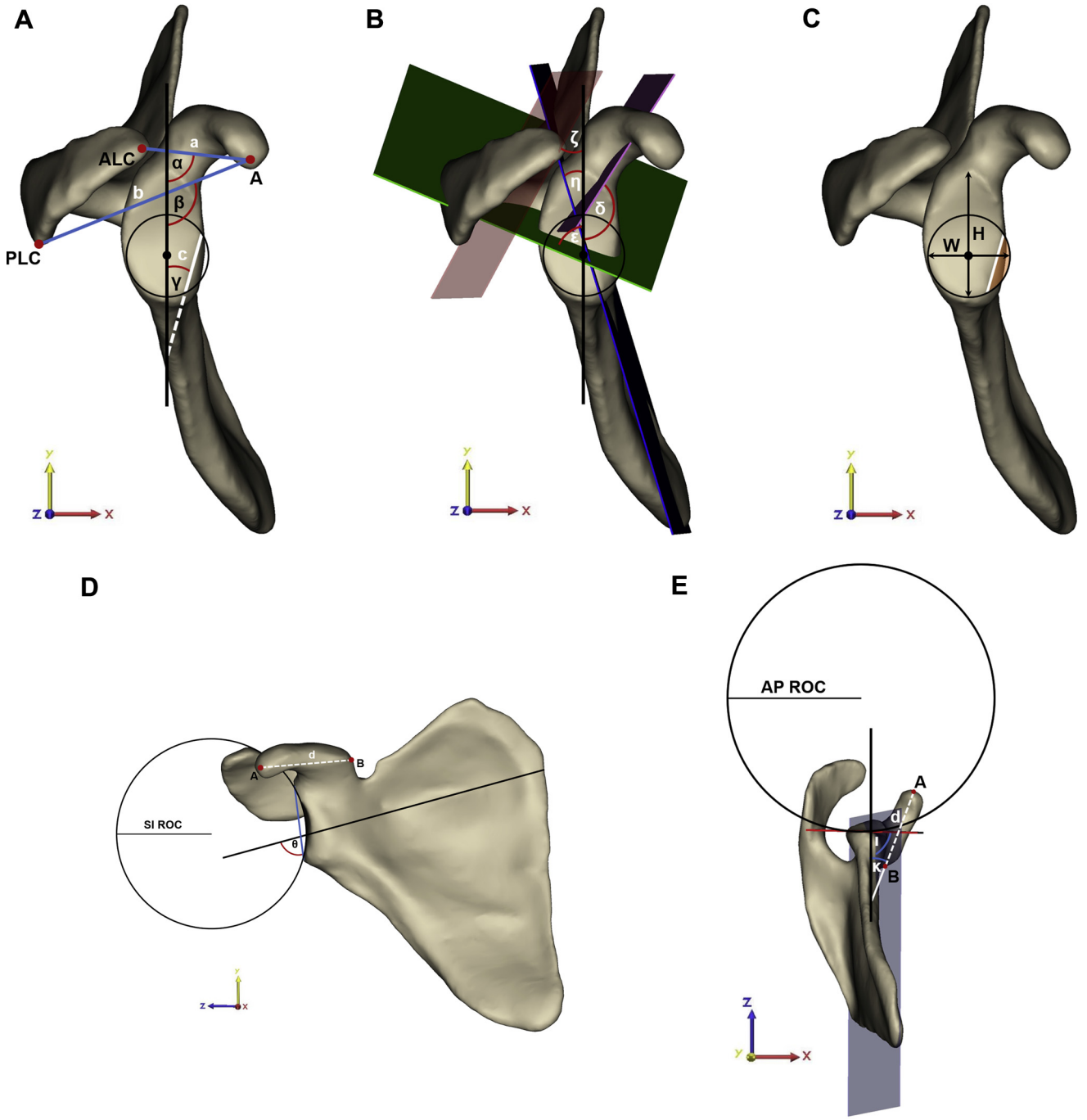

Figure 3 Morphometric measurements were assessed in relation to the center of the best-fit glenoid circle (*O*) (offset measures) and the glenoid center plane (*black line*) (angles). Absolute distances were normalized to the radius of the best-fit glenoid circle for comparison of scapulae of differing sizes. **(A)** The coracoacromial (CA) arch (*a*) and CA base (*b*) distances were determined by the apex of the coracoid process (*A*) and the anterolateral corner (*ALC*) and posterolateral corner (*PLC*) of the acromion, respectively. The CA arch (α) and base angle (β) determined their relationship to the glenoid center plane in the plane of the glenoid. The line tangent to the glenoid defect (*c*) defined the glenoid defect orientation (γ). **(B)** The coracoid pillar angle (δ) and the scapular spine angle (ε) were defined by the plane through the middle of the coracoid pillar (*pink plane*) and scapular spine (*green plane*), respectively. The best-fit plane to the acromion undersurface (*red transparent plane*) determined acromial tilting (ζ). Glenoid tilting (η) was assessed by measuring the angle between the glenoid center plane (*black line*) and the scapular plane (*blue plane*), defined by the center of the glenoid circle (*O*)—the point where the scapular spine intersects the medial border of the scapula (trigonum scapulae) and the most inferior point of the inferior angle of the scapula. **(C)** The glenoid height-width index was calculated by dividing the longitudinal distance of the articular surface of the glenoid along the y-axis (*H*) by the glenoid circle diameter (*W*).[33] Glenoid defect size was calculated as the percentage represented by the missing surface segment with respect to the best-fit glenoid circle (*orange segment*). The equation for the calculation of a circular segment area was

Table I Offset and length measures of coracoid and acromion

	Absolute, mm					Normalized, radii				
	Control group		Unstable group		*P* value	Control group		Unstable group		*P* value
	Mean ± SD	95% CI	Mean ± SD	95% CI		Mean ± SD	95% CI	Mean ± SD	95% CI	
Apex of coracoid										
Anterior	27 ± 3	26-28	26 ± 4	25-27	.532	2.17 ± 0.27	2.07-2.26	2.00 ± 0.30	1.92-2.08	.055
Superior	23 ± 5	21-25	30 ± 4	29-32	<.001*	1.85 ± 0.35	1.72-1.97	2.33 ± 0.37	2.23-2.43	<.001*
Lateral	19 ± 3	18-20	16 ± 4	15-17	<.001*	1.56 ± 0.26	1.47-1.66	1.23 ± 0.38	1.13-1.34	<.001*
Base of coracoid										
Anterior	7 ± 3	6-8	4 ± 3	3-5	<.001*	0.60 ± 0.24	0.51-0.69	0.33 ± 0.21	0.27-0.38	<.001*
Superior	34 ± 4	33-36	34 ± 3	33-35	.935†	2.77 ± 0.38	2.46-2.91	2.62 ± 0.32	2.54-2.71	.047*,†
Lateral	−20 ± 3	−21 to −19	−23 ± 4	−24 to −22	<.001*,†	−1.60 ± 0.20	−1.67 to −1.53	1.74 ± 0.25	−1.81 to −1.67	.002*,†
Coracoid length	45 ± 4	44-57	45 ± 4	44-46	.808	3.69 ± 0.29	3.58-3.79	3.46 ± 0.32	3.37-3.55	.004*,†
CA arch length	40 ± 5	39-42	43 ± 6	41-44	.036*	3.28 ± 0.38	3.14-3.42	3.29 ± 0.46	3.16-3.42	.945
CA base length	69 ± 6	67-71	74 ± 7	72-76	<.001*	5.60 ± 0.46	5.42-5.75	5.66 ± 0.52	5.52-5.80	.543

SD, standard deviation; *CI*, confidence interval; *CA*, coracoacromial.
* Statistically significant.
† Nonparametric Mann-Whitney *U* test.

Discussion

Our hypothesis was confirmed as qualitative SSM-based analysis and quantitative morphometric analysis revealed that coracoid, acromial, and glenoid morphology differ between individuals with and without recurrent traumatic anterior shoulder instability. Specifically, recurrent traumatic anterior shoulder instability was associated with (1) a shorter coracoid process angled more superomedially with a more posterior origin on the glenoid closer to the 12-o'clock position than the 3-o'clock position, (2) a more vertically oriented acromion from a scapular spine with a more posterior origin on the glenoid closer to the 9-o'clock position than the 12-o'clock position, and (3) a more anteriorly tilted glenoid that was flatter in the AP direction with a shape approximating an ellipse rather than a pear. Overall, these morphologic differences demonstrate that traumatic anterior shoulder instability was associated with a more posterior rotation of the CA arch and base. These differences suggest that the CA anatomy may play a potentially important and previously unknown role in glenohumeral stability.

Regarding the coracoid, our study showed increased superomedial offset to both the base and tip of the coracoid, which was shorter and originated more posteriorly on the glenoid. These findings confirm those of Owens et al,[31] who demonstrated that an increasing coracohumeral distance was a risk factor for anterior instability. The importance of the coracoid and its soft tissue is further emphasized by recurrent anterior instability sometimes seen in patients with isolated coracoid fractures.[11,21,39] Coracoid anatomic differences may play a role in glenohumeral instability for multiple reasons. The coracoid and its soft-tissue attachments might act as an anterior buttress to prevent humeral head displacement in the anterior direction. The conjoined tendon might act as a seatbelt, catching the humeral head at the level of the greater tuberosity during anterior shoulder dislocation

used, with the angle between the superior margin of the defect, the origin, and the inferior margin of the defect, as well as the radius of the inferior glenoid circle, being the input variables.[5] **(D)** The distance between the apex (*A*) and base of the coracoid (*B*), formed by the junction of the lateral border of the suprascapular notch with the medial border of the conoid and trapezoid tubercles, provided the coracoid length (*d*).[10] Glenoid inclination (θ), as measured in the coronal plane, was assessed by measuring the angle between the line connecting the superior and inferior glenoid pole (*blue line*) and the scapular axis (*green line*), running through the trigonum scapulae and the center of the glenoid circle. The best-fit circle to the articular surface along the y-axis determined the superior-inferior (*SI*) radius of curvature (*ROC*).[33] **(E)** The following angles were measured in the transverse plane: Glenoid version (ι) was assessed as the angle between the plane of the glenoid (*red line*) and the scapular plane (*blue plane*) on the anterior side of the scapula in the transverse plane. Glenoid version was defined as 90° minus the angle between the scapular plane and the glenoid circle, with a negative value representing retroversion.[19] This measurement differed from that in most studies measuring glenoid version in that the glenoid center plane was used as the reference plane for the coordinate system whereas, in general, the version measurement is made in a coordinate system referring to the scapular plane. The coracoid deviation angle was measured as the angle between the line connecting A and B (*d*) and the glenoid center plane (κ). The anterior-posterior (*AP*) ROC was defined by the best-fit circle to the articular segment posterior to the glenoid center plane along the x-axis.

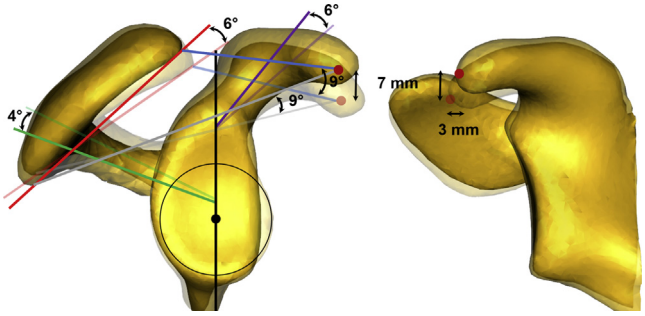

Figure 4 Mean differences between the control group (*transparent*) and unstable group (*solid*) in the coracoacromial (CA) measurements in relation to the glenoid center plane (*black line*), including the coracoid pillar (*purple lines*), scapular spine (*green lines*), acromion (*red lines*), CA arch (*blue lines*), CA base (*gray lines*), and apex of the coracoid process (*red circles*). These differences demonstrate (1) a more superomedially oriented coracoid with a more posteriorly rotated coracoid origin on the glenoid closer to the 12-o'clock position than the 3-o'clock position, (2) a more vertically oriented acromion from a scapular spine with a more posterior origin on the glenoid closer to the 9-o'clock position than the 12-o'clock position, and (3) a more posteriorly rotated CA arch and base. It should be noted that planes were translated to lines for clarification purposes.

motions. In addition, the pathologic position of the coracoid might alter the line of pull of the subscapularis, which is an important shoulder stabilizer.[1,26,40] Hereby, the contact between the conjoined tendon and the subscapularis might be reduced in the low range of motion, leading to an altered line of action of the subscapularis. As a result, glenohumeral compression might be converted into a shear force in a similar but more discrete fashion as seen when transferring the pectoralis major tendon above instead of underneath the conjoined tendon in subscapularis-deficient shoulders.[23] This pathologic anatomy is not addressed by current soft-tissue stabilization procedures and may contribute to recurrence after traumatic anterior shoulder instability in the absence of traditionally defined glenohumeral bone loss. This pathologic anatomy may partially explain the success of the Latarjet procedure, which addresses the pathologic position of the coracoid.[14] However, this nonanatomic procedure overcorrects beyond normal anatomy to obtain a stable shoulder. Our findings regarding the coracoid suggest that there might be a place for more subtle changes of the periarticular structures. A directional osteotomy of the coracoid seems to be the most feasible immediate correction (eg, the Trillat procedure). Adding a coracoid osteotomy to an anatomic procedure such as a capsulolabral repair or bone block procedure potentially better addresses all anatomic lesions associated with glenohumeral instability and may thus increase the success rate of these anatomic procedures. Given that a coracoid osteotomy would be required to correct in multiple directions simultaneously, a freehand technique would likely lack the required precision. Advanced techniques such as application of guiding devices, patient-specific instrumentation, and intraoperative navigation may be required to provide the needed accuracy.

Regarding the acromion, our study showed a posterior origin for the scapular spine and a more vertically oriented acromion. As far as we know, acromial morphology associated with GHJ instability has only been investigated in patients with atraumatic instability.[22] In combination with the altered coracoid morphology, these acromial differences will lead to a more horizontal orientation of the CA ligament. Because the CA ligament has a proven stabilizing function,[15,25,38] acromial differences might also influence shoulder stability. There are multiple potential implications for alterations in acromial and scapular spine anatomy. A more vertically oriented acromion could result in a greater percentage of deltoid muscle posterior to the glenoid center and thus less of the deltoid to resist anterior humeral translation. Similarly, a more posterior origin for the scapula spine could result in a greater percentage of the supraspinatus posterior to the glenoid or a more posterior line of pull for the infraspinatus and teres minor. The pathologic anatomy of the acromion is not addressed by any current stabilization procedures and may contribute to recurrence.

Regarding the glenoid, the glenoid shape in the unstable group was flatter in the AP direction, had a larger H-W index, and was more anteriorly rotated. These findings confirm

Table II Angle measurements of coracoid and acromion

	Control group		Unstable group		*P* value
	Mean ± SD	95% CI	Mean ± SD	95% CI	
Coracoid deviation angle, °	26 ± 4	25-28	29 ± 6	28-31	.013*
Coracoid pillar angle, °	135 ± 7	132-138	141 ± 7	139-143	<.001*
Scapular spine angle, °	61 ± 6	58-63	65 ± 8	63-67	.012*
Acromial tilting, °	49 ± 7	46-52	43 ± 8	41-45	<.001*
CA arch angle, °	78 ± 7	76-81	87 ± 7	85-89	<.001*
CA base angle, °	101 ± 6	99-104	110 ± 6	108-111	<.001*,†

SD, standard deviation; *CI*, confidence interval; *CA*, coracoacromial.
* Statistically significant.
† Nonparametric Mann-Whitney *U* test.

Table III Measurements of glenoid

	Control group		Unstable group		*P* value
	Mean ± SD	95% CI	Mean ± SD	95% CI	
AP ROC, mm	58 ± 45	42-74	135 ± 207	78-191	<.001*,†
SI ROC, mm	35 ± 4	34-37	37 ± 4	36-38	.069
H-W index	1.40 ± 0.096	1.36-1.43	1.44 ± 0.098	1.41-1.46	.021*,†
Version, °	1 ± 3	0-3	2 ± 4	1-3	.114
Anterior tilting, °	17 ± 8	15-20	22 ± 6	20-23	.005*
Inclination, °	84 ± 4	83-86	86 ± 4	85-87	.155

SD, standard deviation; *CI*, confidence interval; *AP*, anterior-posterior; *ROC*, radius of curvature; *SI*, superior-inferior; *H-W*, height-width.
* Statistically significant.
† Nonparametric Mann-Whitney U test.

those of prior studies.[31,33] Hohmann and Tetsworth[17] and Aygün et al[3] found increased anteversion in patients with instability by use of measurements on conventional CT scans. However, Peltz et al[33] and Moroder et al[29] found no difference in glenoid version between patients with traumatic anterior shoulder instability and controls by use of 3D CT scans and multiplanar CT reconstruction in the glenoid center plane, respectively. The differences in glenoid tilt identified in our study explain the discrepancy in the current literature, as version measurements in an anteriorly rotated glenoid will be different on conventional CT scans with 2-dimensional measurements.[27] This highlights the need for standardized measurements on 3D or multiplanar corrected scans, as measurements are then made in predefined planes defined by osseous landmarks. Directional osteotomies around the acromion and/or glenoid might be of biomechanical interest yet less feasible and more invasive, with a lower potential degree of achieved correction, compared with an osteotomy of the coracoid.

Limitations

This study is limited by its retrospective design and the fact that CT scan evaluation is not the standard of care for patients with anterior shoulder instability at our institution. This represents a selection bias and explains the relatively small sample size with a high rate of patients with large defects undergoing the Latarjet procedure. Yet, this retrospective design can be justified because performing a standard CT scan in this young population might raise ethical questions. Although the comparison of several subgroups of instability is of interest, this study was designed to focus on 1 well-defined subgroup to explore whether unknown morphologic differences would be found. Our results provide support to conduct further prospective morphology studies on all types of shoulder instability using CT scans. In addition, the control group was composed of cadaveric shoulders. The average age of this cohort is inherently older than the mean age of patients with traumatic anterior shoulder instability. To be able to match the controls with the pathologic cohort, a younger group of healthy patients should have been acquired. However, this would not exclude potential future shoulder pathology in the control group. Age matching would include young patients in the control group who still might undergo a first-time dislocation later in life, during adulthood, as the typical demography for a first-time dislocation exceeds 1 decade. Moreover, other shoulder pathology including osteoarthritis and rotator cuff tear arthropathy has been related to predisposing scapular shape variation, in particular around the acromion, with acromial measures differing at least 5° and 5 mm between both groups.[4] Although these subjects are asymptomatic at a young age, deterioration toward a pathology later in life is plausible, with the predisposing morphology biasing the analysis substantially. The information provided by donor summaries, dissection, and CT analysis provided us the certainty that the control group had no history of shoulder instability, osteoarthritis, or rotator cuff tear arthropathy. On the other hand, the bone morphology of the cadavers might have been influenced by the aging process. Yet, prior studies have found only small differences or no differences in periarticular anatomy between young and old age groups when comparing corresponding measurements, including glenoid version, lateral offset of the apex of the coracoid process, coracoid deviation angle, and acromial tilt.[7,13,41] In our study, all measures with significant differences between the control and pathologic groups showed larger morphologic differences than those found between different age groups, so we are confident that the revealed differences did not solely rely on an aging process.

Conclusion

Coracoid, acromial, and glenoid anatomy differs between individuals with and without recurrent traumatic anterior shoulder instability. This pathologic anatomy is not addressed by current soft-tissue stabilization procedures and may contribute to recurrence after traumatic anterior shoulder instability in

the absence of traditionally defined glenohumeral bone loss. Although these findings may be difficult to translate to the clinic immediately, they highlight areas on which to focus research relating instability to morphology. The clock-face representation commonly used in shoulder surgery was used as a first step toward clinical application of some measures. More advanced techniques such as navigated surgery and patient-specific instrumentation could also benefit as these 3D measures are integrated into the existing software platforms.

Acknowledgments

The authors acknowledge Spencer Kendell, Savanna Bennett, and Hanna Shluker for their contributions in preparation of 3D model data.

Disclaimer

This study was supported by the L.S. Peery Discovery Program in Musculoskeletal Research (H.B.H. and M.J.); the 10th SECEC/ESSSE (Société Européenne de Chirurgie de l'Epaule et du Coude/European Society for Surgery of the Shoulder and the Elbow) Research Grant 2016 (M.J. and R.Z.T); a grant from the Biomedical Image and Data Analysis Core (H.B.H. and M.J.); the Undergraduate Research Opportunities Program (S.E.B.); and the National Institute of General Medical Sciences of the National Institutes of Health under grant number P41 GM103545-18.

Robert Z. Tashjian is a paid consultant for Cayenne Medical and Mitek; has stock in Conextions, Intrafuse, and Kator; receives intellectual property royalties from Imascap, Shoulder Innovations, and Zimmer; receives publishing royalties from *The Journal of Bone & Joint Surgery*; and serves on the editorial board for the *Journal of Orthopaedic Trauma*. All the other authors, their immediate families, and any research foundations with which they are affiliated have not received any financial payments or other benefits from any commercial entity related to the subject of this article.

Supplementary data

Supplementary data to this article can be found online at https://doi.org/10.1016/j.jse.2019.01.009.

References

1. Ackland DC, Pandy MG. Lines of action and stabilizing potential of the shoulder musculature. J Anat 2009;215:184-97. https://doi.org/10.1111/j.1469-7580.2009.01090.x
2. Atkins PR, Elhabian SY, Agrawal P, Harris MD, Whitaker RT, Weiss JA, et al. Quantitative comparison of cortical bone thickness using correspondence-based shape modeling in patients with cam femoroacetabular impingement. J Orthop Res 2017;35:1743-53. https://doi.org/10.1002/jor.23468
3. Aygün Ü, Çalik Y, Işik C, Şahin H, Şahin R, Aygün DÖ. The importance of glenoid version in patients with anterior dislocation of the shoulder. J Shoulder Elbow Surg 2016;25:1930-6. https://doi.org/10.1016/j.jse.2016.09.018
4. Beeler S, Hasler A, Getzmann J, Weigelt L, Meyer DC, Gerber C. Acromial roof in patients with concentric osteoarthritis and massive rotator cuff tears: multiplanar analysis of 115 computed tomography scans. J Shoulder Elbow Surg 2018;27:1866-76. https://doi.org/10.1016/j.jse.2018.03.014
5. Bhatia S, Saigal A, Frank RM, Bach BR Jr, Cole BJ, Romeo AA, et al. Glenoid diameter is an inaccurate method for percent glenoid bone loss quantification: analysis and techniques for improved accuracy. Arthroscopy 2015;31:608-14.e1. https://doi.org/10.1016/j.arthro.2015.02.020
6. Boileau P, Villalba M, Hery JY, Balg F, Ahrens P, Neyton L. Risk factors for recurrence of shoulder instability after arthroscopic Bankart repair. J Bone Joint Surg Am 2006;88:1755-63. https://doi.org/10.2106/JBJS.E.00817
7. Bouchaib J, Clavert P, Kempf JF, Kahn JL. Morphological analysis of the glenoid version in the axial plane according to age. Surg Radiol Anat 2014;36:579-85. https://doi.org/10.1007/s00276-013-1238-6
8. Brophy RH, Marx RG. Osteoarthritis following shoulder instability. Clin Sports Med 2005;24:47-56. https://doi.org/10.1016/j.csm.2004.08.010
9. Cates J, Fletcher PT, Styner M, Shenton M, Whitaker R. Shape modeling and analysis with entropy-based particle systems. Inf Process Med Imaging 2007;20:333-45.
10. Chahla J, Marchetti DC, Moatshe G, Ferrari MB, Sanchez G, Brady AW, et al. Quantitative assessment of the coracoacromial and the coracoclavicular ligaments with 3-dimensional mapping of the coracoid process anatomy: a cadaveric study of surgically relevant structures. Arthroscopy 2018;34:1403-11. https://doi.org/10.1016/j.arthro.2017.11.033
11. Chammaa R, Miller D, Datta P, McClelland D. Coracoid stress fracture with late instability. Am J Sports Med 2010;38:2328-30. https://doi.org/10.1177/0363546510371370
12. Cicchetti DV, Sparrow SA. Developing criteria for establishing interrater reliability of specific items: applications to assessment of adaptive behavior. Am J Ment Defic 1981;86:127-37.
13. Dugarte AJ, Davis RJ, Lynch TS, Schickendantz MS, Farrow LD. Anatomic study of subcoracoid morphology in 418 shoulders: potential implications for subcoracoid impingement. Orthop J Sports Med 2017;5. 2325967117731996. https://doi.org/10.1177/2325967117731996
14. Giles JW, Boons HW, Elkinson I, Faber KJ, Ferreira LM, Johnson JA, et al. Does the dynamic sling effect of the Latarjet procedure improve shoulder stability? A biomechanical evaluation. J Shoulder Elbow Surg 2013;22:821-7. https://doi.org/10.1016/j.jse.2012.08.002
15. Gohlke F, Janssen E, Leidel J, Heppelmann B, Eulert J. Histomorphological findings on proprioception in the shoulder. Orthopade 1998;27:510-7.
16. Harris MD, Datar M, Whitaker RT, Jurrus ER, Peters CL, Anderson AE. Statistical shape modeling of cam femoroacetabular impingement. J Orthop Res 2013;31:1620-6. https://doi.org/10.1002/jor.22389

17. Hohmann E, Tetsworth K. Glenoid version and inclination are risk factors for anterior shoulder dislocation. J Shoulder Elbow Surg 2015; 24:1268-73. https://doi.org/10.1016/j.jse.2015.03.032
18. Horst K, Von Harten R, Weber C, Andruszkow H, Pfeifer R, Dienstknecht T, et al. Assessment of coincidence and defect sizes in Bankart and Hill-Sachs lesions after anterior shoulder dislocation: a radiological study. Br J Radiol 2014;87:20130673. https://doi.org/10.1259/bjr.20130673
19. Jacxsens M, Van Tongel A, Henninger HB, Tashjian RZ, De Wilde L. The three-dimensional glenohumeral subluxation index in primary osteoarthritis of the shoulder. J Shoulder Elbow Surg 2017;26:878-87. https://doi.org/10.1016/j.jse.2016.09.049
20. Jacxsens M, Van Tongel A, Willemot LB, Mueller AM, Valderrabano V, De Wilde L. Accuracy of the glenohumeral subluxation index in nonpathologic shoulders. J Shoulder Elbow Surg 2015;24:541-6. https://doi.org/10.1016/j.jse.2014.07.021
21. Kennedy NI, Ferrari MB, Godin JA, Sanchez G, Provencher MT. Repair of an isolated coracoid fracture with suture anchor fixation. Arthrosc Tech 2017;6:E1715-9. https://doi.org/10.1016/j.eats.2017.06.042
22. Kondo T, Hashimoto J, Nobuhara K, Takakura Y. Radiographic analysis of the acromion in the loose shoulder. J Shoulder Elbow Surg 2004;13:404-9. https://doi.org/10.1016/S1058274604000199
23. Konrad GG, Sudkamp NP, Kreuz PC, Jolly JT, McMahon PJ, Debski RE. Pectoralis major tendon transfers above or underneath the conjoint tendon in subscapularis-deficient shoulders. An in vitro biomechanical analysis. J Bone Joint Surg Am 2007;89:2477-84. https://doi.org/10.2106/JBJS.F.00811
24. Kroner K, Lind T, Jensen J. The epidemiology of shoulder dislocations. Arch Orthop Trauma Surg 1989;108:288-90.
25. Lee TQ, Black AD, Tibone JE, McMahon PJ. Release of the coracoacromial ligament can lead to glenohumeral laxity: a biomechanical study. J Shoulder Elbow Surg 2001;10:68-72.
26. Lee SB, Kim KJ, O'Driscoll SW, Morrey BF, An KN. Dynamic glenohumeral stability provided by the rotator cuff muscles in the mid-range and end-range of motion. A study in cadavera. J Bone Joint Surg Am 2000;82:849-57.
27. Matsumura N, Oki S, Suzuki T, Iwamoto T, Sato K, Nakamura M, et al. A computed tomography analysis of three-dimensional glenoid orientation modified by glenoid torsion. JSES Open Access 2018;2: 194-9. https://doi.org/10.1016/j.jses.2018.07.002
28. Milano G, Grasso A, Russo A, Magarelli N, Santagada DA, Deriu L, et al. Analysis of risk factors for glenoid bone defect in anterior shoulder instability. Am J Sports Med 2011;39:1870-6. https://doi.org/10.1177/0363546511411699
29. Moroder P, Ernstbrunner L, Pomwenger W, Oberhauser F, Hitzl W, Tauber M, et al. Anterior shoulder instability is associated with an underlying deficiency of the bony glenoid concavity. Arthroscopy 2015;31:1223-31. https://doi.org/10.1016/j.arthro.2015.02.009
30. Olds M, Ellis R, Donaldson K, Parmar P, Kersten P. Risk factors which predispose first-time traumatic anterior shoulder dislocations to recurrent instability in adults: a systematic review and meta-analysis. Br J Sports Med 2015;49:913-22. https://doi.org/10.1136/bjsports-2014-094342
31. Owens BD, Campbell SE, Cameron KL. Risk factors for anterior glenohumeral instability. Am J Sports Med 2014;42:2591-6. https://doi.org/10.1177/0363546514551149
32. Owens BD, Duffey ML, Nelson BJ, DeBerardino TM, Taylor DC, Mountcastle SB. The incidence and characteristics of shoulder instability at the United States Military Academy. Am J Sports Med 2007;35:1168-73. https://doi.org/10.1177/0363546506295179
33. Peltz CD, Zauel R, Ramo N, Mehran N, Moutzouros V, Bey MJ. Differences in glenohumeral joint morphology between patients with anterior shoulder instability and healthy, uninjured volunteers. J Shoulder Elbow Surg 2015;24:1014-20. https://doi.org/10.1016/j.jse.2015.03.024
34. Provencher MT, Bhatia S, Ghodadra NS, Grumet RC, Bach BR Jr, Dewing CB, et al. Recurrent shoulder instability: current concepts for evaluation and management of glenoid bone loss. J Bone Joint Surg Am 2010;92(Suppl 2):133-51. https://doi.org/10.2106/JBJS.J.00906
35. Robinson CM, Howes J, Murdoch H, Will E, Graham C. Functional outcome and risk of recurrent instability after primary traumatic anterior shoulder dislocation in young patients. J Bone Joint Surg Am 2006;88:2326-36. https://doi.org/10.2106/JBJS.E.01327
36. Shaha JS, Cook JB, Rowles DJ, Bottoni CR, Shaha SH, Tokish JM. Clinical validation of the glenoid track concept in anterior glenohumeral instability. J Bone Joint Surg Am 2016;98:1918-23. https://doi.org/10.2106/JBJS.15.01099
37. Shaha JS, Cook JB, Song DJ, Rowles DJ, Bottoni CR, Shaha SH, et al. Redefining "critical" bone loss in shoulder instability: functional outcomes worsen with "subcritical" bone loss. Am J Sports Med 2015;43:1719-25. https://doi.org/10.1177/0363546515578250
38. Su WR, Budoff JE, Luo ZP. The effect of coracoacromial ligament excision and acromioplasty on superior and anterosuperior glenohumeral stability. Arthroscopy 2009;25:13-8. https://doi.org/10.1016/j.arthro.2008.10.004
39. Subramanian AS, Khalik MA, Shah MM. Isolated fracture of the coracoid process associated with unstable shoulder. ANZ J Surg 2007; 77:188-9. https://doi.org/10.1111/j.1445-2197.2006.04005.x
40. Turkel SJ, Panio MW, Marshall JL, Girgis FG. Stabilizing mechanisms preventing anterior dislocation of the glenohumeral joint. J Bone Joint Surg Am 1981;63:1208-17.
41. Vahakari M, Leppilahti J, Hyvonen P, Ristiniemi J, Paivansalo M, Jalovaara P. Acromial shape in asymptomatic subjects: a study of 305 shoulders in different age groups. Acta Radiol 2010;51:202-6. https://doi.org/10.3109/02841850903476556

Table S1 Reliability of measurements

	Inter-rater reliability		Intrarater reliability		TEM
	ICC	95% CI	ICC	95% CI	
Absolute offset and length measures					
Apex of coracoid					
Anterior	0.809	0.638-0.904	0.810	0.639-0.904	0.62
Superior	0.949	0.884-0.976	0.984	0.968-0.993	0.45
Lateral	0.949	0.895-0.975	0.994	0.988-0.997	0.43
Base of coracoid					
Anterior	0.875	0.756-0.938	0.920	0.839-0.961	0.51
Superior	0.642	0.272-0.829	0.721	0.458-0.862	0.79
Lateral	0.832	0.627-0.922	0.905	0.811-0.953	0.58
Coracoid length	0.977	0.952-0.989	0.985	0.945-0.995	0.25
CA arch length	0.932	0.841-0.969	0.955	0.903-0.979	0.68
CA base length	0.941	0.880-0.972	0.947	0.891-0.974	0.64
Normalized offset and length measures					
Apex of coracoid					
Anterior	0.765	0.547-0.883	0.779	0.587-0.888	0.048
Superior	0.910	0.819-0.956	0.956	0.911-0.979	0.045
Lateral	0.943	0.884-0.972	0.992	0.983-0.996	0.036
Base of coracoid					
Anterior	0.883	0.770-0.942	0.927	0.852-0.965	0.039
Superior	0.706	0.243-0.877	0.791	0.496-0.908	0.063
Lateral	0.751	0.528-0.875	0.812	0.645-0.906	0.048
Coracoid length	0.879	0.763-0.940	0.863	0.734-0.932	0.045
CA arch length	0.895	0.702-0.956	0.926	0.836-0.965	0.053
CA base length	0.891	0.772-0.948	0.912	0.823-0.957	0.071
Periarticular angle measures					
Coracoid deviation angle	0.826	0.663-0.913	0.966	0.925-0.984	0.99
Coracoid pillar angle	0.778	0.587-0.888	0.878	0.763-0.940	1.38
Scapular spine angle	0.921	0.838-0.962	0.969	0.936-0.985	1.04
Acromial tilting	0.904	0.647-0.964	0.991	0.980-0.996	1.02
CA arch angle	0.938	0.875-0.970	0.984	0.966-0.992	0.87
CA base angle	0.953	0.905-0.977	0.997	0.994-0.999	0.61
Glenoid measures					
AP ROC	0.866	0.740-0.934	0.924	0.849-0.963	4.20
SI ROC	0.874	0.668-0.946	0.919	0.791-0.965	0.66
H-W index	0.817	0.622-0.912	0.775	0.579-0.886	0.017
Version	0.902	0.806-0.952	0.950	0.897-0.976	0.50
Anterior tilting	0.971	0.939-0.986	0.980	0.957-0.990	0.48
Inclination	0.944	0.887-0.973	0.980	0.934-0.992	0.45

ICC, intraclass correlation coefficient; *CI*, confidence interval; *TEM*, typical error of measurement; *CA*, coracoacromial; *AP*, anterior-posterior; *ROC*, radius of curvature; *SI*, superior-inferior; *H-W*, height-width.